

## TECHNICAL NOTE

# Functional Assessment of Lumbar Nerve Roots Using Coronal-plane Single-shot Turbo Spin-echo Diffusion Tensor Imaging

Takayuki Sakai<sup>1,2\*</sup>, Yasuchika Aoki<sup>3,4</sup>, Atsuya Watanabe<sup>3,4</sup>, Masami Yoneyama<sup>5</sup>, Shigehiro Ochi<sup>1</sup>, and Tosiaki Miyati<sup>2</sup>

We investigated the usefulness of diffusion tensor imaging using single-shot turbo spin-echo sequence (TSE–DTI) in detecting the responsible nerve root by multipoint measurements of fractional anisotropy (FA) values. Five patients with bilateral lumbar spinal stenosis showing unilateral neurological symptoms were examined using TSE–DTI. In the spinal canal, FA values in the symptomatic side were lower than those in the asymptomatic side. TSE–DTI using multipoint measurements of FA values can differentiate the responsible lumbar nerve root.

**Keywords:** *diffusion tensor imaging, fractional anisotropy, lumbar nerve roots, lumbar spinal stenosis*

## Introduction

The MRI of low back pain with representative symptoms is a useful diagnostic tool for evaluating the origin of pain experienced by a patient.

Conventional MRI examination can be used to evaluate neural tissue compressions in the spinal canal; however, it cannot diagnose the lumbar nerve root compression in the extraforaminal area. Diffusion tensor imaging (DTI) based on a single-shot echo planar imaging sequence (i.e., EPI–DTI) can detect the water molecule diffusion along the nerve fibers in neural tissues and is a promising method for evaluating lumbar nerve root compression in the extraforaminal area.<sup>1</sup> Several studies that used EPI–DTI recently showed that tractography can visualize the lumbar nerves, and the degree of lumbar nerve damage was quantitatively evaluated using fractional anisotropy (FA) by identifying the preferential water molecule diffusion.<sup>2</sup> These previous studies on EPI–DTI indicated that the FA values decreased in the presence of peripheral nerve compression with nerve damage because of neurodegeneration, such as interstitial space widening, Wallerian degeneration,

and axonal demyelination, which induces increased perpendicular diffusion vector compared with the normal nerves.<sup>3</sup>

Although EPI–DTI has great potential for the evaluation of lumbar nerve compression, several problems, such as long acquisition times in obtaining a sufficient signal-to-noise ratio (SNR) using multiple signal averages, geometric distortion, and artifact susceptibility due to its high sensitivity to magnetic susceptibility, were observed. Therefore, we proposed a new quantitative method for evaluating lumbar nerve disorders using DTI with a single-shot turbo spin-echo sequence (i.e., TSE–DTI) to reduce image distortion.<sup>4</sup>

The cause of neurological symptoms in the lower extremities remains controversial because the imaging and clinical findings are inconsistent in some patients. For example, lumbar spinal stenosis is a disease that causes symptoms mainly on the lower extremities because of nerve compression; however, in clinical settings, patients often experience a significant narrowing of the spinal canal without neurological symptoms on their lower extremities.

Some patients also have unilateral neurological symptoms on the lower extremities and bilateral lumbar spinal stenosis on MRI images, whereas others have lumbar spinal stenosis on multiple levels and unilateral lower extremity symptoms owing to one-level responsible nerve root. Therefore, the diagnostic ability of MRI in differentiating between symptomatic and asymptomatic nerve roots should be improved as much as possible in clinical practice. Although several previous studies that used EPI–DTI for the lumbar nerve roots have already been conducted in patients with lumbar spinal stenosis,<sup>5</sup> no study has investigated the inconsistencies between imaging and clinical findings. Therefore, this study aimed to investigate whether TSE–DTI, which decreases image distortion, is useful in detecting the responsible nerve root

<sup>1</sup>Department of Radiology, Eastern Chiba Medical Center, 3-6-2 Okayamadai, Togane, Chiba 283-8686, Japan

<sup>2</sup>Division of Health Sciences, Graduate School of Medical Sciences, Kanazawa University, Kanazawa, Japan

<sup>3</sup>Department of General Medical Services, Graduate School of Medicine, Chiba University, Chiba, Japan

<sup>4</sup>Department of Orthopedic Surgery, Eastern Chiba Medical Center, Chiba, Japan

<sup>5</sup>Philips Japan, Tokyo, Japan

\*Corresponding author, Phone: +81-475-50-1199, Fax: +81-475-50-1356, E-mail: sakai@tkmedical.jp

©2019 Japanese Society for Magnetic Resonance in Medicine

This work is licensed under a Creative Commons Attribution-NonCommercial-NoDerivatives International License.

Received: January 28, 2019 | Accepted: May 9, 2019

by quantitatively evaluating the nerve damage on multi-point measurements in patients with bilateral lumbar spinal stenosis and unilateral neurological symptoms on their lower extremities.

## Materials and Methods

All patients were examined using a 1.5T whole-body clinical system (Ingenia, Philips Healthcare, Best, The Netherlands). DTI analyses were performed using Ziostation2 (AMIN, Tokyo, Japan) for tractography depiction and FA value measurements. Statistical analyses were performed using IBM SPSS statistics version 23.0 (IBM, Armonk, NY, USA). The Institutional Review Board approved the study, and written informed consents were obtained from all patients.

### Initial clinical study

We selected five patients with bilateral lumbar spinal stenosis who exhibited discrepancies between clinical and MRI findings from among 35 patients who underwent MRI examination including TSE–DTI for low back pain or neurological symptoms in the lower extremities between April 2015 and December 2015. A spinal surgeon diagnosed the spinal canal stenosis which was defined based on the results of MRI as follows: central stenosis with the thecal sac measuring <100 mm<sup>2</sup> in area, obliteration of perineural fat and compression of lateral recess or foramen, and ligament hypertrophy. The lumbar nerve roots (L<sub>4</sub>–S<sub>1</sub> levels) of five patients (mean age: 69.8; age range: 65–76 years) with bilateral lumbar spinal stenosis and unilateral neurological symptom on their lower extremities were examined using TSE–DTI and 3D-balanced steady-state free precession (SSFP) as a reference image for anatomical structure. Table 1 shows the patient summary. The symptom-responsible level in patient summary was diagnosed on the basis of the clinical and MRI findings as well as results of nerve root block, which is an injection of local anesthetic by a spinal surgeon into the region where the nerve exits the spinal column.

**Table 1** Patient summary

Patient no.	Age	Sex	Responsible level and side	Symptoms
1	76	Male	Left L <sub>5</sub>	Numbness in a lower leg and dysuria
2	74	Female	Left L <sub>5</sub>	Sciatica
3	68	Male	Left L <sub>5</sub>	Leg pain
4	65	Female	Left L <sub>5</sub>	Leg pain and numbness in the hip
5	66	Male	Right L <sub>4</sub>	Numbness in a lower leg

### Imaging parameters

Diffusion tensor imaging using single-shot turbo spin-echo sequence was acquired using parallel imaging methods known as sensitivity encoding (SENSE) with a factor of three and spectral selective fat suppression. The phase-encoding direction was right-to-left, and phase oversampling was used to prevent aliasing artifacts. The following imaging parameters were used: motion probing gradient (MPG) of 32 directions; *b*-value of 400 s/mm<sup>2</sup>; TR and TE of 3000 and 49 ms; echo train length, including a phase oversampling of 24; coronal slice orientation, slice thickness, and slice gap of 4.0 and 0 mm; FOV of 350 × 350 mm<sup>2</sup>; matrices of 88 × 88; actual voxel size of 3.98 × 3.98 × 4.0 mm<sup>3</sup>; calculated voxel size of 1.56 × 1.56 × 4.0 mm<sup>3</sup>; two excitations; 16 slices; and an acquisition time of 6 min and 36 s.

A 3D-balanced SSFP was acquired using spectral selective fat suppression and SENSE with factors of 1.2 for the phase direction and 1.2 for the slice direction. The phase-encoding direction was right-to-left, and phase oversampling was used to prevent aliasing artifacts. The following imaging parameters were used: TR and TE of 5.5 and 2.8 ms, respectively; axial slice orientation; slice thickness and slice gap of 1.2 and 0.6 mm, respectively; FOV of 160 × 160 mm<sup>2</sup>; matrices of 240 × 240; actual voxel size of 0.67 × 0.67 × 1.2 mm<sup>3</sup>; calculated voxel size of 0.31 × 0.31 × 1.2 mm<sup>3</sup>; shot duration of 500 ms; shot interval of 1500 ms; flip angle of 40°; one excitation; 180 slices; and acquisition time of 5 min and 40 s.

### Assessment methods

The FA value was measured on the FA map obtained from the DTI at and adjacent to the symptom-responsible level that was diagnosed on the basis of the nerve root block results assessed by a spinal surgeon. The actual measurement procedure of the FA values is as follows: First, the FA map was superimposed on the 3D-balanced SSFP image, and the course of a nerve root was determined. Subsequently, the FA values of both lumbar nerve roots were measured in an axial plane perpendicular to the spine, in which the ROIs were set on the fusion image with a 3D-balanced SSFP image. Regarding the measurement points, the nerve roots were divided into 18 points at 2.4 mm intervals from the upper edge height of the intervertebral disc to the nerve ganglion for evaluation from the cauda equina in the spinal canal to the dorsal root ganglion in the extraforaminal area (Fig. 1). The FA values were evaluated as follows: (1) Mean FA values of both nerve roots at the symptom-responsible level, (2) mean FA values of both nerve roots on normal levels, and (3) changes in FA values on 18 measurement points by making line graphs for visual comparison of left and right nerve roots. The difference in FA values between the nerve roots was statistically evaluated using the Wilcoxon test. Values of *P* < 0.05 were considered statistically significant. Regarding “(3) changes in FA values on 18 measurement points,” we defined

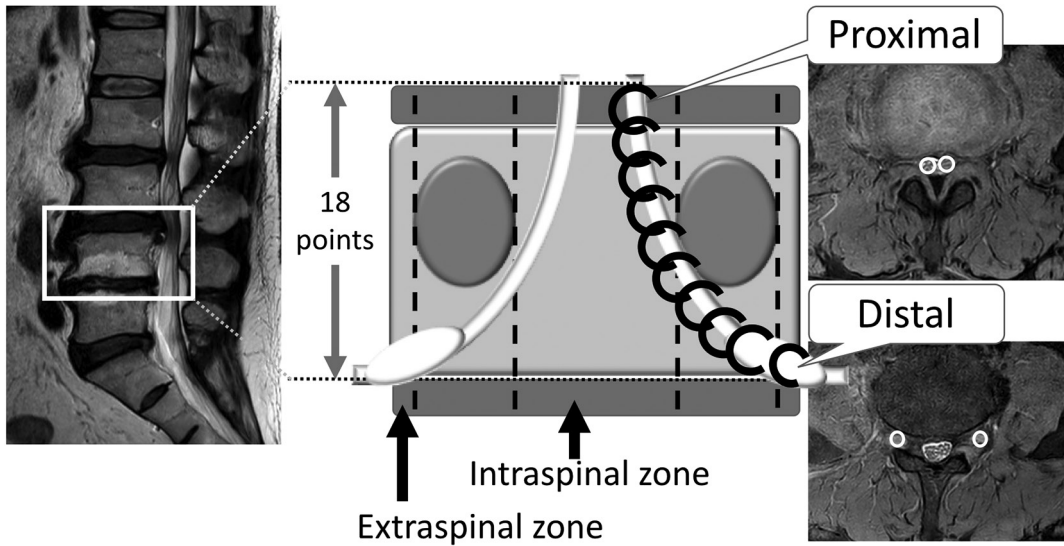


**Fig. 1** ROI setting of the fractional anisotropy value measurement. Fractional anisotropy (FA) values were continuously measured at 18 points both proximally and distally to the bilateral lumbar foraminal zone at and adjacent to the symptom-responsible level.

regional change rate of FA values using the following equation to evaluate the amount of change in FA values:

$$\text{Regional change rate of FA values (\%)} = \frac{\text{Regional maximum FA value distal to the point of minimum FA value / minimum FA value}}{\text{Point number}} \times 100$$

## Results

### Assessment of mean FA values in five patients

Figure 2 shows the results of the mean FA values on both nerve roots at the symptom-responsible and normal levels. No significant difference was observed in the mean FA values of the both nerve roots at the normal level, whereas the mean FA values in the symptomatic side were significantly lower than those in the asymptomatic side at the symptom-responsible level ( $P < 0.05$ ). The mean FA values in the symptomatic side at the symptom-responsible level were significantly lower than those in both nerve roots at the normal levels ( $P < 0.05$ ).

### Assessment of FA values on multipoint measurements

Figures 3–6 show the results in four patients on multipoint measurements of FA values at the symptom-responsible and normal levels. Plotting line graphs of the FA values on multipoint measurements and visually comparing the graph shapes of the left and right nerve roots at each level revealed the following. All nerve roots showed a tendency that the FA values gradually increase from proximal to distal. At the normal level, the line-graphs of the left and right FA values showed similar shapes, which were simply continuously increasing. At the symptom-responsible level, the FA values in the symptomatic side tended to be lower than those in the asymptomatic side. The difference in FA values between the left and right sides was evident

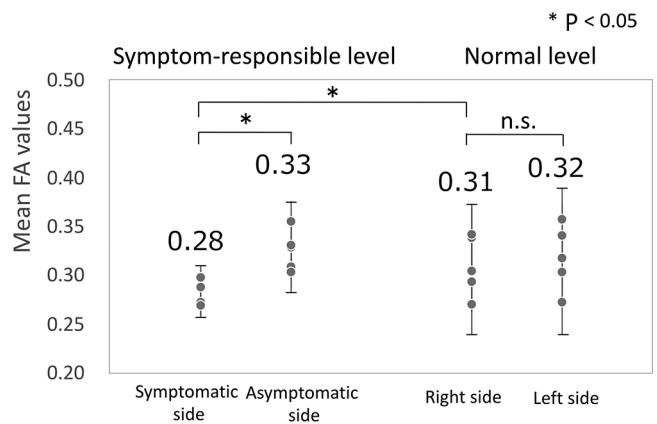
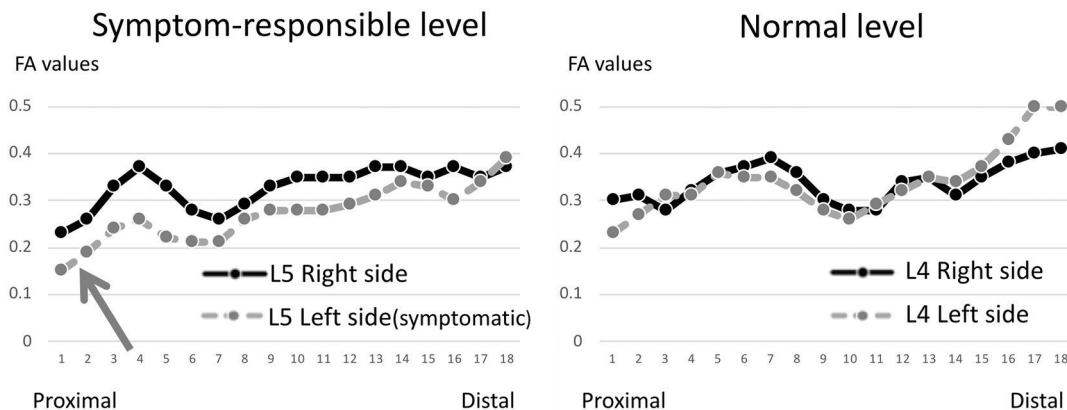


**Fig. 2** Comparison of mean fractional anisotropy values between the left and right sides. Mean FA values on both nerve roots at symptom-responsible and normal levels. FA, fractional anisotropy; n.s., not significant.

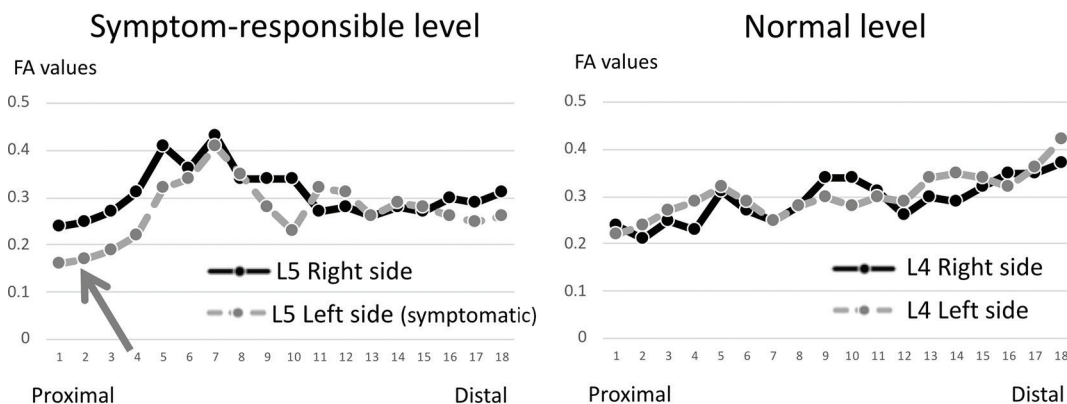
in the spinal canal, and the FA values in the symptomatic side were lower than those in the asymptomatic side (Figs. 3–5). Furthermore, at the symptom-responsible level, the FA value locally increased at the position distal to the points where the FA value is lower than the asymptomatic side. The FA values also tended to gradually decrease thereafter.

Figure 7 shows the results in a patient on multipoint measurements of FA values. At the symptom-responsible level, the FA values in the symptomatic side were remarkably lower than those in the asymptomatic side at two measurement points. Tractography showed nerve root compression at the points corresponding to the two measurement points, thus suggesting that nerve root compression caused the lower extremity symptoms.

Table 2 shows the results of the regional change rate of FA values. The regional change rates of FA values on the symptomatic side were higher than those on the asymptomatic



**Fig. 3** Multipoint measurements of the fractional anisotropy values. Line-graph of FA values of a 76-year-old patient (patient 1) on multipoint measurements at symptom-responsible and normal levels. Arrow shows the point of minimum FA value where the area of responsible lumbar nerve root lesion is present. FA, fractional anisotropy.



**Fig. 4** Multipoint measurements of the fractional anisotropy values. Line-graph of FA values of a 74-year-old patient (patient 2) on multipoint measurements at the symptom-responsible and normal levels. Arrow shows the point of minimum FA value where the area of responsible lumbar nerve root lesion is present. FA, fractional anisotropy.

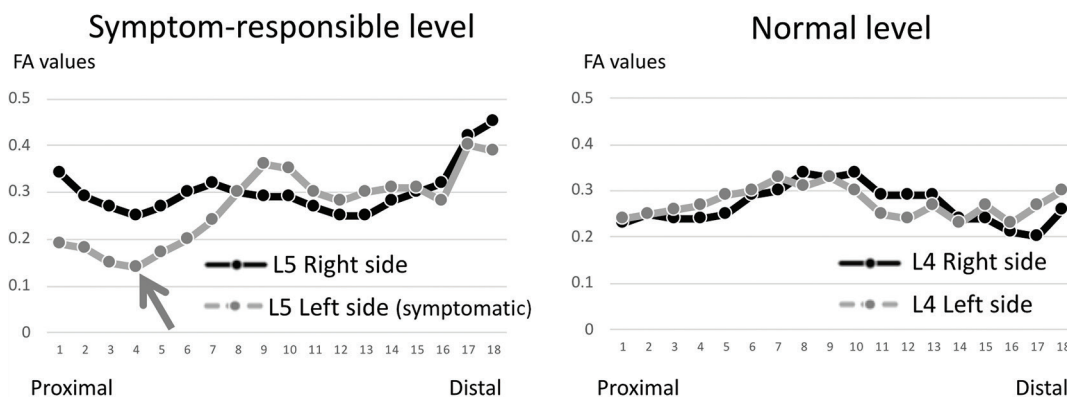


**Fig. 5** Multipoint measurements of the fractional anisotropy values. Line-graph of FA values of a 68-year-old patient (patient 3) on multipoint measurements at the symptom-responsible and normal levels. Arrow shows the point of minimum FA value where the area of responsible lumbar nerve root lesion is present. FA, fractional anisotropy.

side. For patient 1, the regional change rates of FA values on both sides were almost the same, but FA values in the measured section on the symptomatic side were severely lower than those on the asymptomatic side.

### Discussion

On the basis of the mean FA values of five patients at the symptom-responsible level, the mean FA values in the

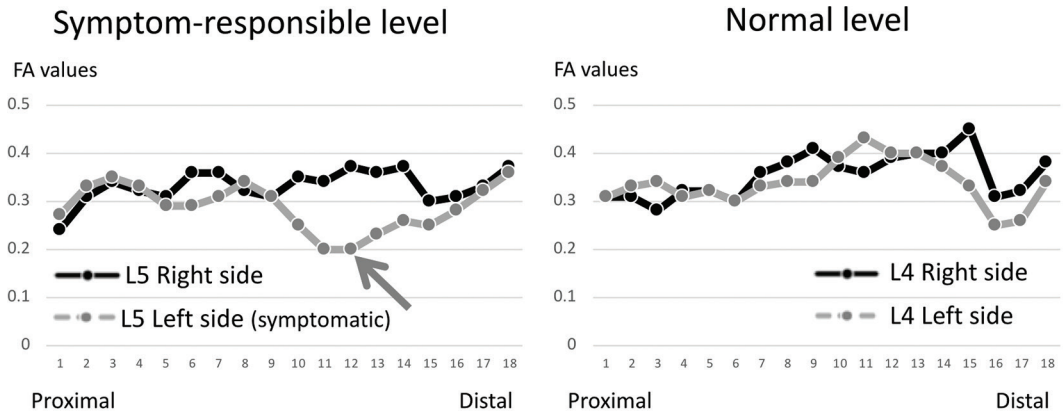


**Fig. 6** Multipoint measurements of the fractional anisotropy values. Line-graph of FA values of a 65-year-old patient (patient 4) on multipoint measurements at the symptom-responsible and normal levels. Arrow shows the point of minimum FA value where the area of responsible lumbar nerve root lesion is present. FA, fractional anisotropy.

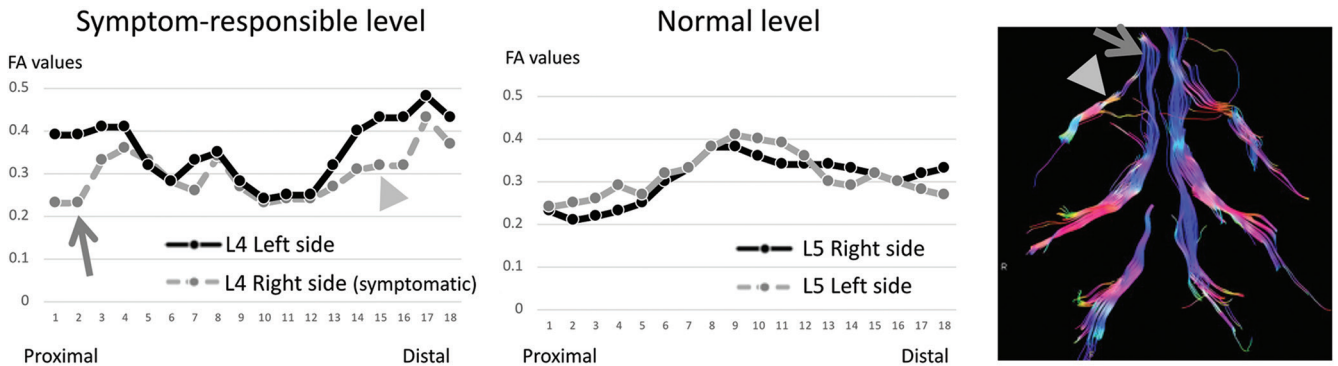


**Fig. 7** Multipoint measurements of the FA values and tractography visualization. Line-graph of FA values of a 66-year-old patient (patient 5) on multipoint measurements at symptom-responsible and normal levels and the tractography. At the symptom-responsible level, the FA values in the symptomatic side were remarkably lower than those in the asymptomatic side at two measurement points (arrow and arrowhead). Tractography showed nerve root compression at the points corresponding to the two measurement points (arrow and arrowhead), thus suggesting that nerve root compression caused the lower extremity symptoms. FA, fractional anisotropy.

**Table 2** Regional change rate of FA values (%)

Patient no.	Symptom-responsible level			Normal level		
	Point no.	Symptomatic side	Asymptomatic side	Point no.	Right side	Left side
1	1–4	43.3	40.2	1–7	18.6	21.7
2	1–7	36.6	25.6	1–5	25.8	29.1
3	4–9	42.9	19.3	1–9	18.4	19.0
4	11–18	22.5	13.6	1–9	14.7	12.2
5	1–4	39.1	26.3	1–7	18.6	19.6

symptomatic side was shown to be significantly lower than those in the asymptomatic side. Some cases must have multi-level or bilateral nerve root compression in which the responsible nerve root was not determined using conventional MRI examination; however, TSE-DTI can potentially differentiate the side responsible for the symptoms and quantitatively evaluate the nerve damage.

Fractional anisotropy value changes were visually observed according to the FA values on multipoint measurement graphs. The FA values tended to increase toward the distal side of the nerve roots, which is similar to the results in other previous studies.<sup>6</sup> At the normal level, the line-graph shape of FA values is similar between the left and right sides; at the symptom-responsible level, those in the symptomatic

side was different from those in the asymptomatic side because the FA values were lower at the nerve damage points. Given that the FA values particularly decreased at a region in the spinal canal with nerve compression owing to lumbar spinal stenosis, TSE–DTI may contribute to determining the damaged nerve root points. At the symptom-responsible levels, the FA values were found to locally increase at the areas just distal to the point with decreased FA values due to nerve damage. A previous study reported the possible explanation of this finding that the FA values increase when the nerve root is compressed by disk herniation or ligament thickening but without nerve damage.<sup>7</sup> As shown in Table 2, regional change rate on the symptomatic side tends to increase more than that on the asymptomatic side. The FA values decreased once at nerve damage points, but increased at the distal side because of the presence of normal nerves. Therefore, the regional change rate of FA values on the symptomatic side showed a steeper shape than that on the asymptomatic side on the line graphs. This shows that a steep shape on the line graphs might be an indicator of nerve damage. On the other hand, the results of patient 1 (Fig. 3 and Table 2) showed a similar graph shape and regional change rate of FA values on the left and right sides. However, because the minimum FA value on the symptomatic side is clearly low, it would be possible to distinguish the symptomatic side. The FA values change significantly depending on the presence or absence of nerve damage. Pathologically, the regional decrease in FA values indicates not only neurodegeneration such as inflammation, edema, interstitial space widening, and Wallerian degeneration but also conditions such as axonal demyelination and axonal injury.<sup>8</sup> On the other hand, in case of compression of nerve roots without nerve damage, the FA values would increase due to densely packed nerve fibers. Therefore, the dynamic FA value changes could be observed by sequentially evaluating the symptomatic nerve roots and were used to determine the presence or absence of neurological symptom. Furthermore, Fig. 7 shows two lesions with nerve damage, thus indicating lumbar foraminal stenosis and lumbar spinal stenosis. Considering that the degree of nerve root damage could be visually observed by showing the FA values on multipoint measurements graph, this method may further contribute to the identification of the nerve damage point that caused the lower extremity symptoms. Therefore, we would like to conclude that patients with lumbar degenerative disease should be clinically evaluated using FA values, particularly the multipoint measurements, because the FA values of nerve roots dynamically fluctuate according to the degree of nerve damage.

In this study, a DTI technique with low distortion was introduced on the basis of the TSE–DWI sequence by direct coronal acquisition and was used to evaluate the lumbar nerve roots in patients with bilateral spinal canal stenosis with unilateral neurological symptoms. Theoretically, TSE can minimize the geometric distortion because of its insensitivity to magnetic field inhomogeneity compared with EPI;<sup>9</sup>

therefore, the improved reproducibility of FA value measurement is expected. The results show that TSE–DTI can be used effectively to estimate nerve damage sites that cannot be detected using conventional MRI imaging.

Our study has several limitations. The first limitation is the low spatial resolution associated with TSE–DTI; therefore, high SNR should be maintained using a low spatial resolution. The actual voxel size of TSE–DTI used in this study was 4.0 mm<sup>3</sup>, whereas the lumbar nerve root diameter is usually <4.0 mm<sup>2</sup>. Therefore, the quantitative values in TSE–DTI, such as the FA values, might be inaccurate because of the partial volume effect in evaluating narrow nerves with <4.0 mm<sup>2</sup>. The cauda equina nerve is densely distributed in the spinal canal because of lumbar spinal stenosis; therefore, the nerve root in the spinal canal might be affected by the partial volume in this study. High-spatial-resolution TSE–DTI is required to accurately and quantitatively evaluate nerve damage. Nevertheless, the FA value on the symptomatic and asymptomatic sides could be distinguished with a significant difference in this study because the cauda equina in the spinal canal was densely packed owing to bilateral spinal canal stenosis. In the ROIs, in addition to the cauda equina, the surrounding tissues such as cerebrospinal fluid, blood vessels, bones, and muscles are located close to the nerve root, particularly in the case of lumbar spinal stenosis. However, given that the diffusion anisotropy in the surrounding tissues was lower than that of the cauda equina, the FA values would not be affected as much as expected. The second limitation is the small number of patients with TSE–DTI. To understand the usefulness of lumbar nerve root evaluation and the variance among the patients evaluated with TSE–DTI, further studies are needed to determine whether our findings remain valid in a large number of patients. The third limitation is the low SNR associated with TSE–DTI. The measurement accuracy of FA values would be affected by the SNR of source images.<sup>10</sup> For maintaining a relatively high SNR with TSE–DTI, we used the *b*-value of 400 s/mm<sup>2</sup> in this study; TSE–DTI set at this *b*-value includes not only the water molecular diffusion but also the effects of perfusion, such as blood flow through capillaries. Previous studies have shown that the *b*-value slightly affects the DTI parameters.<sup>11</sup> Hence, the accuracy of the FA values obtained using TSE–DTI should be further investigated clinically.

In the future, imaging methods in TSE–DTI should be improved, and a high-magnetic-field machine such as a 3T MRI should be used to improve SNR. Considering that a previous study has reported the usefulness of high-spatial-resolution DTI in evaluating lumbar nerve roots,<sup>12</sup> we believe that the increasing SNR in TSE–DTI enables high-spatial-resolution DTI with reduced image distortion; this approach would improve the accuracy and reproducibility of quantitative evaluations using DTI in diagnosing nerve damage. Consequently, our method is expected to help in the clinical diagnosis of patients with lumbar degenerative disease with lower extremity symptoms.

## Conclusion

A DTI technique with low distortion was introduced on the basis of the TSE–DWI sequence, and the lumbar nerve roots in patients with bilateral lumbar spinal stenosis with unilateral neurological symptoms in the lower extremities were evaluated using TSE–DTI. TSE–DTI effectively differentiated the responsible lumbar nerve root lesions quantitatively and visually using the multipoint measurements of FA values. It can also be used to estimate the responsible nerve roots and help diagnose lumbar degenerative diseases because of its insensitivity to magnetic field inhomogeneity and ability to reduce image distortion.

## Conflicts of Interest

The authors declare that they have no conflicts of interest.

## References

- Mukherjee P, Chung SW, Berman JJ, Hess CP, Henry RG. Diffusion tensor MR imaging and fiber tractography: technical considerations. *AJNR Am J Neuroradiol* 2008; 29:843–852.
- Li J, Wang Y, Wang Y, Lv Y, Ma L. Study on lumbosacral nerve root compression using DTI. *Biomed Rep* 2016; 5:353–356.
- Khalil C, Budzik JF, Kermarrec E, Balbi V, Le Thuc V, Cotten A. Tractography of peripheral nerves and skeletal muscles. *Eur J Radiol* 2010; 76:391–397.
- Sakai T, Doi K, Yoneyama M, Watanabe A, Miyati T, Yanagawa N. Distortion-free diffusion tensor imaging for evaluation of lumbar nerve roots: utility of direct coronal single-shot turbo spin-echo diffusion sequence. *Magn Reson Imaging* 2018; 49:78–85.
- Kanamoto H, Eguchi Y, Suzuki M, et al. The diagnosis of double-crush lesion in the L5 lumbar nerve using diffusion tensor imaging. *Spine J* 2016; 16:315–321.
- Eguchi Y, Ohtori S, Suzuki M, et al. Discrimination between lumbar intraspinal stenosis and foraminal stenosis using diffusion tensor imaging parameters: preliminary results. *Asian Spine J* 2016; 10:327–334.
- Sakai T, Miyagi R, Yamabe E, Fujinaga Y, Bhatia NN, Yoshioka H. Diffusion-weighted imaging and diffusion tensor imaging of asymptomatic lumbar disc herniation. *J Med Invest* 2014; 61:197–203.
- Shen J, Zhou CP, Zhong XM, et al. MR neurography: T1 and T2 measurements in acute peripheral nerve traction injury in rabbits. *Radiology* 2010; 254:729–738.
- De Foer B, Vercruyse JP, Pilet B, et al. Single-shot, turbo spin-echo, diffusion-weighted imaging versus spin-echo-planar, diffusion-weighted imaging in the detection of acquired middle ear cholesteatoma. *AJNR Am J Neuroradiol* 2006; 27:1480–1482.
- Farrell JA, Landman BA, Jones CK, et al. Effects of signal-to-noise ratio on the accuracy and reproducibility of diffusion tensor imaging-derived fractional anisotropy, mean diffusivity, and principal eigenvector measurements at 1.5 T. *J Magn Reson Imaging* 2007; 26:756–767.
- Wu Y, Zou C, Liu W, et al. Effect of B-value in revealing postinfarct myocardial microstructural remodeling using MR diffusion tensor imaging. *Magn Reson Imaging* 2013; 31:847–856.
- Kanamoto H, Eguchi Y, Oikawa Y, et al. Visualization of lumbar nerves using reduced field of view diffusion tensor imaging in healthy volunteers and patients with degenerative lumbar disorders. *Br J Radiol* 2017; 90:20160929.